You might find this additional information useful...

This article cites 32 articles, 17 of which you can access free at:
http://ajpheart.physiology.org/cgi/content/full/286/5/H1742#BIBL

This article has been cited by 5 other HighWire hosted articles:

Analysis of cardiac mitochondrial Na+-Ca2+ exchanger kinetics with a biophysical model of mitochondrial Ca2+ handing suggests a 3: 1 stoichiometry
R. K. Dash and D. A. Beard
J. Physiol., July 1, 2008; 586 (13): 3267-3285.
[Abstract] [Full Text] [PDF]

Principal strain changes precede ventricular wall thinning during transition to heart failure in a mouse model of dilated cardiomyopathy
J. H. Hankiewicz, P. H. Goldspink, P. M. Buttrick and E. D. Lewandowski
Am J Physiol Heart Circ Physiol, January 1, 2008; 294 (1): H330-H336.
[Abstract] [Full Text] [PDF]

Limiting sarcolemmal Na+ entry during resuscitation from ventricular fibrillation prevents excess mitochondrial Ca2+ accumulation and attenuates myocardial injury
S. Wang, J. Radhakrishnan, I. M. Ayoub, J. D. Kolarova, D. M. Taglieri and R. J. Gazmuri
J Appl Physiol, July 1, 2007; 103 (1): 55-65.
[Abstract] [Full Text] [PDF]

Compartmentation of cAMP Signaling in Cardiac Myocytes: A Computational Study
R. V. Iancu, S. W. Jones and R. D. Harvey
Biophys. J., May 1, 2007; 92 (9): 3317-3331.
[Abstract] [Full Text] [PDF]

Oxidative ATP synthesis in skeletal muscle is controlled by substrate feedback
F. Wu, J. A. L. Jeneson and D. A. Beard
Am J Physiol Cell Physiol, January 1, 2007; 292 (1): C115-C124.
[Abstract] [Full Text] [PDF]

Updated information and services including high-resolution figures, can be found at:
http://ajpheart.physiology.org/cgi/content/full/286/5/H1742

Additional material and information about *AJP - Heart and Circulatory Physiology* can be found at:
http://www.the-aps.org/publications/ajpheart

This information is current as of December 12, 2008 .

Myocardial density and composition: a basis for calculating intracellular metabolite concentrations

Kalyan C. Vinnakota and James B. Bassingthwaighte
Department of Bioengineering, University of Washington, Seattle, Washington 98195

Vinnakota, Kalyan C., and James B. Bassingthwaighte. Myocardial density and composition: a basis for calculating intracellular metabolite concentrations. *Am J Physiol Heart Circ Physiol* 286: H1742–H1749, 2004. First published December 23, 2003; 10.1152/ ajpheart.00478.2003.—Systems for describing myocardial cellular metabolism with appropriate thermodynamic constraints on reactions have to be on the basis of estimates of intracellular and mitochondrial concentrations of metabolites as driving forces for reactions. This requires that tissue composition itself must be modeled, but there is marked inconsistency in the literature and no full data set on hearts of any species. To formulate a self-consistent set of information on the densities, contents, or concentrations of chemical components and volumes of tissue spaces, we drew on information mostly on rats. From the data on densities, volumes, volume fractions, and mass fractions observed mainly on left ventricular myocardium, cytoplasm, and mitochondria and from morphometric data on cellular components and the vasculature, we constructed a matrix based on conservation laws for density, volume, and constituent composition. The four constituents were water, protein, fat, and solutes (or ash). To take into account the variances in the observed data sets, we used a constrained nonlinear least squares optimization to minimize the differences between the final results and the data sets. The results provide a detailed estimate of cardiac tissue composition, previously unavailable, for the translation of whole tissue concentrations or concentrations per gram protein into estimated local concentrations that are relevant to reaction processes. An example is that the concentrations of phosphocreatine and ATP in cytosolic water space are twice as high as their mean tissue concentrations. This conservation optimization method is applicable to any tissue or organ.

heart tissue; water content; cellular energetics; metabolic modeling

CURRENTLY THERE IS NO self-consistent set of data on the composition of the myocardium in terms of water, protein, fat, and solutes at both tissue and subcellular levels. Accurate compositional data are needed to calculate the concentrations of metabolically active substances to know their thermodynamic potentials accurately. This is important, because it is the concentrations that drive reactions, transport, and signaling processes that govern cell function. Experimentally, the metabolite concentrations in a piece of tissue are measured in units that are independent of region volume, such as nanomoles per gram dry weight of tissue or micromoles per gram protein. With estimates of metabolite volumes of distribution, that is, the water spaces in the tissue or in the subcellular regions, one can translate volume-independent units of metabolite quantities into thermodynamically effective concentrations.

Although there are some published data on tissue composition in the literature, e.g., in books (4, 5) and articles (9, 25, 35), there are no data sets that reconcile observations on mass, volume, density, tissue component fractions, and water content. Yipintsoi et al. (39) devised a three-component composition diagram that forced adherence to conservation laws for mass, volume, and density. In their analysis of the composition of dog ventricular myocardium at the whole tissue level, the authors considered the major constituents of water, fat, and tissue solids. Tissue solids were protein, including structural components of cells and tissue, and other molecular solutes. Taking a similar stance, in a recent review, Aliev et al. (2) calculated the probable distribution of water in rat hearts at the levels of whole tissue and intracellular composition. They considered only water and dry solids as the constituents, so although this was on the right track, it does not give enough detail to allow calculation of regional or subcellular concentrations that are normalized with respect to tissue or cell protein. To obtain the composition of all of the major regions of myocardium, we *1*) developed a set of equations for tissue composition, based on four constituents (water, protein, fat, and small solutes) that distinguish multiple regions in the tissue down to the subcellular level; *2*) solved the equations by integrating data on rat heart composition from diverse sources; and *3*) computed the precision of the best estimates by use of a Monte Carlo simulation. Data used to solve the equations include the quantitative morphometry of cellular dimensions, estimates of intracellular water distribution by X-ray microanalysis, and tissue water space measurement by tracer dilution, density measurements on tissues, component densities, and subcellular elements.

We have also taken into account that whole heart density is different than the density of myocardial tissue from which large vessels have been removed. Even after the major coronary arteries and veins are removed, tissue includes some vascular space, namely, capillaries and small blood vessels. Ideally, from the point of view of where metabolism occurs, we would define nutrient flow as the flow per unit extravascular space, as recommended by Bassingthwaighte et al. (7) and Prinzen and Bassingthwaighte (30). By such a definition, all blood content of tissue would be excluded, because it is not a part of the metabolizing tissue; in reality, tissue samples do contain capillary blood, and so we compromise by defining tissue as the extravascular tissue plus the microvascular space.

METHODS OF DATA ACQUISITION AND ANALYSIS

Simultaneous consideration of many observations from various studies using different techniques (densities, mass fractions, volume fractions) requires developing of sets of simultaneous equations and

solving them to determine a self-consistent set of information integrated under the constraints that mass, volume, and density are explicitly physically related. This means also that all unmeasured parameters of tissue and subcellular composition are defined within the same context, and we can benefit from having their constraint-based estimates.

The equations are all mass and volume balance expressions. All spaces in a piece of tissue are assumed to be composed of the four constituents: fat, protein, water, and small molecular solutes, which have the same densities in the various regions.

The cells are mainly cardiomyocytes with ~1–2% endothelial cells plus small fractions of smooth muscle, fibroblasts, neuronal endings, etc., but we put them together. This means that we introduce small errors because endothelial cells have few mitochondria and less myofilament protein and are less dense than muscle cells. For the purpose of generating a self-consistent set of compositional data of heart tissue, we considered the tissue regions with the generic subscript r in the heart, as listed in Table 1, to be the vascular space, divided into plasma (pl) and red blood cell (RBC) spaces, the interstitial fluid (ISF), and the generic cell. The whole heart is defined as myocardial tissue plus large superficial blood vessels.

Table 1 gives a list of symbols and definitions. Each region, whether the whole organ, a particular component of the tissue, or a component of the cell, is composed of the four constituents, so that their relative fractions define the measurable variables, density, mass, and volume. From these numbers we derived the volume fractions and the mass fractions. Because we included blood contained in the microvasculature (small arterioles, capillaries, and venules), we recognized that hematocrit decreases with vessel diameter (24, 29, 32) and attempted to account for reductions in hematocrit and density in small vessels and the microvascular network. These influenced the estimates of whole tissue mass, density, and water content. Although the vascular volume is small, this matters because RBCs are relatively dry and therefore dense ($\rho_{RBC} = 1.097$ g/ml) (5, 14).

Equations for Mass and Volume Balances in Heart Tissue

The approach was to use conservation expressions for the purpose of making all the regional estimates self consistent with the whole. This makes the estimates interdependent, because any error in one estimate must be balanced by compensatory errors in other estimates.

By minimizing the numbers of classes of constituents and of classes of regions as described in Table 1, we minimized complexity and maximized the ratio of observed data to unknowns.

Mass conservation relations. Mass conservation relations for the components of the whole heart give rise to a set of equations. The heart mass is the sum of the components' mass fractions

$$\rho_{heart}V_{heart} = \rho_{RBC}V_{RBC} + \rho_{pl}V_{pl} + \rho_{ISF}V_{ISF} + \rho_{cell}V_{cell} = 1 \text{ g/g} \quad (1)$$

where V_r is volume (ml/g heart), ρ_r is density (g/ml), and cell is the generic cell, so that the mass fraction for each component is ρ_rV_r and the sum is $\rho_{heart}V_{heart} = 1$ g/g.

The constituents of the heart are fat, protein, water, and solutes, all of which have mass fraction in the heart defined by

$$C_{heart}(\text{g/g}) = \sum_r \rho_rV_rC_r \quad (2)$$

where C_r denotes the mass fraction of the constituent (C) in the region (r) in units of gram per gram, where r = large vessel, microcirculation, ISF, and generic cell, as in *Eq. 1*, and the summation gives the mass of constituent in grams per gram of heart. The constituent mass fractions of fat (F), protein (P), water (W), and solutes (S) in each region always sum to unity within each region

$$1 = P_r + F_r + W_r + S_r, \text{ g/g} \quad (3)$$

as do the fractions for the whole heart

$$1 = P_{heart} + F_{heart} + W_{heart} + S_{heart}, \text{ g/g} \quad (4)$$

Volume conservation relations. On the basis of the assumption that the volumes of the constituents of a physical tissue or cellular space are additive, a set of volume conservation equations can be written for all such physical spaces, remembering that $V_{heart} = 1/\rho_{heart}$

$$V_{heart} = \sum_r V_r, \text{ ml/g heart} \quad (5)$$

$$\frac{1}{\rho_r} = \frac{P_r}{\rho_P} + \frac{F_r}{\rho_F} + \frac{W_r}{\rho_W} + \frac{S_r}{\rho_S}, \text{ ml/g region} \quad (6)$$

where we have assumed that volumes are additive. For solutes, this implies an average partial molar volume of unity. Brozek et al. (9), in

Table 1. *Symbols and definitions*

Symbol	Definition	Units
r	Denotes a particular region and takes the following values.	Unitless
	At organ level	
	Heart, meaning the whole of the organ	
	LV, blood in large blood vessels >100 μm in diameter in rats	
	tiss, Tissue: heart minus the large vessels	
	micro, Blood in microcirculation, vessel diameter < 100 μm in rats	
	pl, Plasma: whole organ plasma space	
	RBC, red blood cell: whole organ RBC space	
	ISF, interstitial fluid space	
	Cell, cellular space: meaning the whole of the cell	
	At subcellular level	
	mi, Mitochondria	
	SR, sarcoplasmic reticulum	
	cy, Cytosol, includes sarcoplasm, myofibrils, and subcellular spaces other than mi and SR	
C	Denotes a particular constituent and takes the following values for all regions r	Unitless
	P (protein), with density $\rho_P = 1.34$ g/ml. (9)	
	W (water), with density $\rho_W = 0.994$ g/ml at 37°C. (9)	
	F (fat), with density $\rho_F = 0.901$ g/ml. (3)	
	S (solute), with density $\rho_S = 3.32$ g/ml. (9)	
ρ_r	Density of region r	g/ml
ρ_c	Density of constituent C	g/ml
V_r	Volume of r per gram of tissue	ml/g tissue
C_r	Mass fraction of C in r	g/g
C_r'	Volume fraction of C in r	ml/ml
Hct	Hematocrit (defined for LV and microvascular regions)	Dimensionless

Table 2. *Input data*

Parameter	Value	Units	Species	References
W'_{RBC}	0.67 (0.015)	ml/ml	Dog	14
RBC fat	510 (51)	mg/100 ml RBC		28
W'_{mi}	0.725	ml/ml	Rat	34
W'_{cy}	0.845	ml/ml	Rat	34
Plasma water	0.946 (0.007)	g/ml	Rat	5
Plasma protein	0.06 (0.01)	g/ml	Rat	5
ISF water	0.153 (0.011)	g/g heart	Rat	13
P_{heart}	0.1758	g/g heart	Rat	Calculated
F_{heart}	0.0205	g/g heart	Guinea pig	12
S_{heart}	0.0137	g/g tissue	Rat	Calculated
W_{heart}	0.79 (0.012)	g/g heart	Rat	13
ρ_{RBC}	1.097 (0.002)	g/ml	Multiple	5
ρ_{pl}	1.024 (0.002)	g/ml	Rat	5
ρ_{mi}	1.1	g/ml	Rat	26
ρ_{cy}	1.055	g/ml	Rat	34
Mitochondrial protein	0.053 (0.001)	g/g tiss	Rat	20
SR protein	29.2	mg/ml cytosol		8
V_{mi}/V_{cell}	0.32 (0.032)	Dimensionless	Rat	6
V_{SR}/V_{cell}	0.035 (0.002)	Dimensionless	Rat	27
V_{cy}/V_{cell}	0.645	Dimensionless	Rat	$1 - (V_{mi}/V_{cell} + V_{SR}/V_{cell})$
ρ_P	1.34	g/ml		9
ρ_F	0.901	g/ml		3
ρ_W	0.9937	g/ml		9
ρ_S	3.317	g/ml		9
V_{LV}/V_{micro}	0.1395	ml/ml	Rat	21
Hct_{LV}	0.45	Dimensionless	Rat	13
$Hct_{tiss} = 0.8\ Hct_{LV}$	0.36	Dimensionless	Rat	29
$\rho_{pl}V_{pl}W_{pl}$	0.059 (0.007)	g/g heart	Rat	13
$\rho_{RBC}V_{RBC} + \rho_{pl}V_{pl}$	0.106 (0.011)	g/g heart	Rat	13
Plasma albumin	0.035 (0.001)	g/ml plasma	Rat	37
ISF albumin	0.017	g/ml ISF	Rat	37

Values in parentheses are standard deviations. ρ_{RBC}, RBC density; ρ_{pl}, plasma density; ρ_{mi}, mi density; ρ_{cy}, cy density; W'_{RBC}, RBC water fraction; W'_{mi}, mi water fraction; W'_{cy}, cy water fraction; V, volume; cell, generic cell.

arriving at an apparent small molecular solute density of 3.32 g/ml, took into account the partial molar volumes of the solutes.

Composition diagrams. The four constituent fractions of heart can be mapped as a tetrahedral four-constituent composition diagram with four apices that are the pure constituents with their particular and known densities. For display purposes in this presentation, we reduced the tetrahedron to a planar triangular plot by putting together protein and solutes. This works well, because their weighted combined density is 1.40 (3) calculated from 1.34 g/ml for protein and 3.32 g/ml (9) for salts at a constant ratio, $P_{tiss}/S_{tiss} = 12.91$, taking this for the rat data in Table 2, resulting in the calculated mass fractions that are to be found in RESULTS in Table 3. The densities ρ_P and ρ_s are strikingly different from those of water and fat, and in the lumped representation, the density is closer to that of protein. The composition diagram provides a map of density wherein each point describes the fraction of these three components in the tissue. (On a tetrahedral map

of protein, fat, water, and solute, this assumption would be unnecessary, and the calculations would be more accurate.)

Figure 1 is a composition diagram, a three-constituent phase plot using protein + solute, water, and fat as the three vertices. The normal myocardial point, with a density of 1.053 g/ml, is what is to be calculated from our algorithms below. Dehydration of the tissue is represented by a straight line moving directly away from the 100% water apex from the normal point. Edema is represented by moving from the normal point directly toward the 100% water point. A line of constant density, unachievable in reality, is given by the straight line labeled 1.053 g/ml.

Equations for Mass and Volume Balances in the Cell

The subcellular regions are the mitochondria (mi), myofibrillar and sarcoplasmic spaces together known as cytoplasm (cy), and sarcoplas-

Table 3. *Rat myocardial tissue regional densities, volumes, and constituent mass fractions*

Region	Density g/ml	Volume ml/(g tissue)	Water Fraction g/(g region)	Protein Fraction g/(g region)	Fat Fraction g/(g region)	Solute Fraction g/(g region)
Tissue	1.053 (0.05)	0.95 (0.06)	0.79 (0.23)	0.176 (1)	0.02 (1)	0.014 (1.5)
Plasma	1.023 (0.2)	0.056 (12.8)	0.924 (0.2)	0.059 (0.2)	0.002 (28)	0.015 (17.2)
RBC	1.097 (0.2)	0.033 (36.4)	0.67 (1.9)	0.308 (6.3)	0.004 (0.2)	0.018 (43.9)
ISF	1.022 (0.85)	0.167 (8.3)	0.924 (2.8)	0.065 (38.9)	0.001 (29)	0.01 (83.6)
Cell (total)	1.06 (0.17)	0.694 (2.5)	0.755 (0.41)	0.204 (1.4)	0.028 (2.64)	0.014 (14.8)
Cytoplasm	1.044 (0.31)	0.472 (3.9)	0.807 (0.31)	0.17 (5.6)	0.019 (34.4)	0.004 (78.3)
Mitochondria	1.09 (0.81)	0.2 (7.6)	0.664 (0.71)	0.25 (7.3)	0.048 (26)	0.036 (24.4)
SR	1.137 (0.18)	0.024 (2.6)	0.518 (1.5)	0.445 (0.18)	0.021 (31.2)	0.016 (16.5)

Values in parentheses are coefficients of variation in percent. ISF, interstitial fluid.
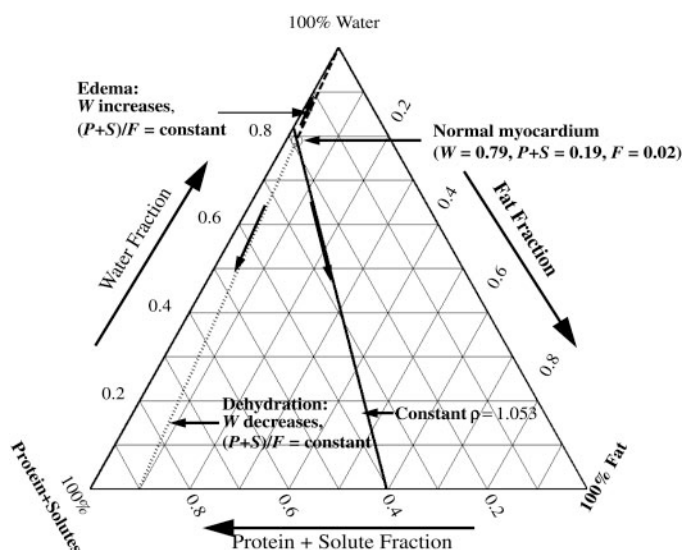
Fig. 1. Three-constituent composition plots of myocardial tissue. The vertex W is pure water with a density (ρ) of 0.994 g/ml; the vertex F is fat with a density of 0.90 ml/g, and the third vertex P + S is protein plus dissolved small molecular solutes with a combined density of ~1.40 g/ml. The myocardial composition is given by the point normal myocardium, with a density of 1.053 g/ml.

mic reticulum (sr). The equation for the cellular mass fraction, in terms of the subcellular regions, is

$$\rho_{cell}V_{cell} = \rho_{cy}V_{cy} + \rho_{mi}V_{mi} + \rho_{sr}V_{sr}, \text{g/(g heart)} \qquad (7)$$

and for a specific constituent

$$\rho_{cell}V_{cell}C_{cell}(\text{g/g}) = \sum_{r} \rho_{r}V_{r}C_{r} \qquad (8)$$

where r = mi, cy, and sr.

The volume balance equations at the cellular level are similar to *Eqs. 6* and *7*

$$V_{cell} = \sum_{r} V_{r}, \text{ml/(g heart)} \qquad (9)$$

and within each subcellular region

$$\frac{1}{\rho_{r}} = \frac{P_{r}}{\rho_{P}} + \frac{F_{r}}{\rho_{F}} + \frac{W_{r}}{\rho_{W}} + \frac{S_{r}}{\rho_{S}}, \text{ml/(g region)} \qquad (10)$$

For the system of *Eqs. 1–10*, the unknowns are protein, fat, solute, and water for mitochondria, cytoplasm, and sarcoplasmic reticulum regions and the densities (ρ_{sr} and ρ_{cell}). Values for ρ_{mi} and ρ_{cy} are known from data. Values for these variables are listed in Table 2.

Solution of the Mass Balance and Volume Balance Equations

The sets of *Eqs. 1–10* contain 42 individual variables. We have data on 15 individual variables and eight quantities that are expressed as combinations of some of the variables (Table 2). These eight quantities expressed as combinations of some of variables constitute eight constraint equations in addition to the mass and volume balance equations. Additional constraint equations were added to keep the solutions positive. The variables are all of the mass and volume fractions, and the regional and global densities. The parameters are the values for ρ_{C}, the constituent densities.

The known quantities (listed in Table 2) taken from the literature have standard deviations that have to be mapped to the unknown variables. This was achieved by solving the balance equations and the constraint equations using the "fsolve" function in Matlab, in con-

junction with a Monte Carlo simulation. In each iteration, values of the known quantities were drawn from log-normal distributions with the first moment equal to the reported mean and the second moment about the mean equal to the reported variance. These were then used in the solution of the sets of equations developed. The fsolve function was set up so that solutions that converge to a local minimum that are not roots of the specified equations are rejected. From a large number of such iterations, sets of feasible solutions were obtained, and their sample statistics were taken.

Initial guesses were obtained by using a spreadsheet to solve the above 10 equations approximately by adjusting the constituent mass and volume fractions of all regions to predict the known quantities as closely as possible. For example, the volume fractions of cellular organelles were taken from stereological estimates; the water volume fractions in myofibrils and mitochondria were taken from X-ray microanalysis (34). These were inputs to the spread sheet. Included also were densities of the constituent components and the hematocrits in the large vessels and microvasculature.

RESULTS

The optimization to obtain the most likely set of volumes, mass fractions, and densities used analysis that has been applied to the data listed in Table 2, including the standard deviations of the observations. Table 3 summarizes the results and shows density, volume, and composition of whole organ and subcellular regions in terms of the component mass fractions. Figure 2 shows the shapes of the probability density functions of the estimated values listed in Table 3. To emphasize the great range of constituent compositions in different regions, these data are plotted on the "composition" diagram in Fig. 3, where the plot shows only the upper apex of the diagram in Fig. 1. Plasma and ISF are close together and about one-half the distance from the "normal tissue" point to the water apex, 100% water. Cytoplasmic composition is close to that of the whole tissue and has 80% water. RBC and mitochondria are relatively dry (~67% and 66% water) and relatively dense (1.097 and 1.1 g/ml).

Cell values show that the tissue is only 69% cells by volume, 0.69 ml/g, including all cell types. The remaining 31% of the tissue includes the vasculature, providing nutrients and removing metabolites, and the structural materials of the ISF. The total cell interior is high in protein, and although the cytoplasmic protein mass fraction is only 17%, the mitochondrial protein fraction is higher (0.25 g/g).

High protein fractions are in mitochondria and RBC, and the highest estimated are in sarcoplasmic reticulum. In RBC, the protein is mainly hemoglobin, the prime constituent of its cytoplasm. In sarcoplasmic reticulum, it is presumably sarco-(endo)plasmic reticulum Ca^{2+}-ATPase, which makes up ~80% of its membrane-bound protein (8), combined with Ca-calsequestrin in the lumen that accounts for the high density, a density higher even than that of mitochondria.

Solute fractions of plasma, ISF, and cell were all just >0.01 g/g. These are unconstrained estimates. The lack of constraining data, coupled with the fact that the amounts are small and do not influence other mass fraction estimates significantly, leads to the large values of their coefficients of variation.

Total Organ Values

If the arteries and veins were included within a "total organ," then the average organ density would be 1.0527 [0.06% coef-
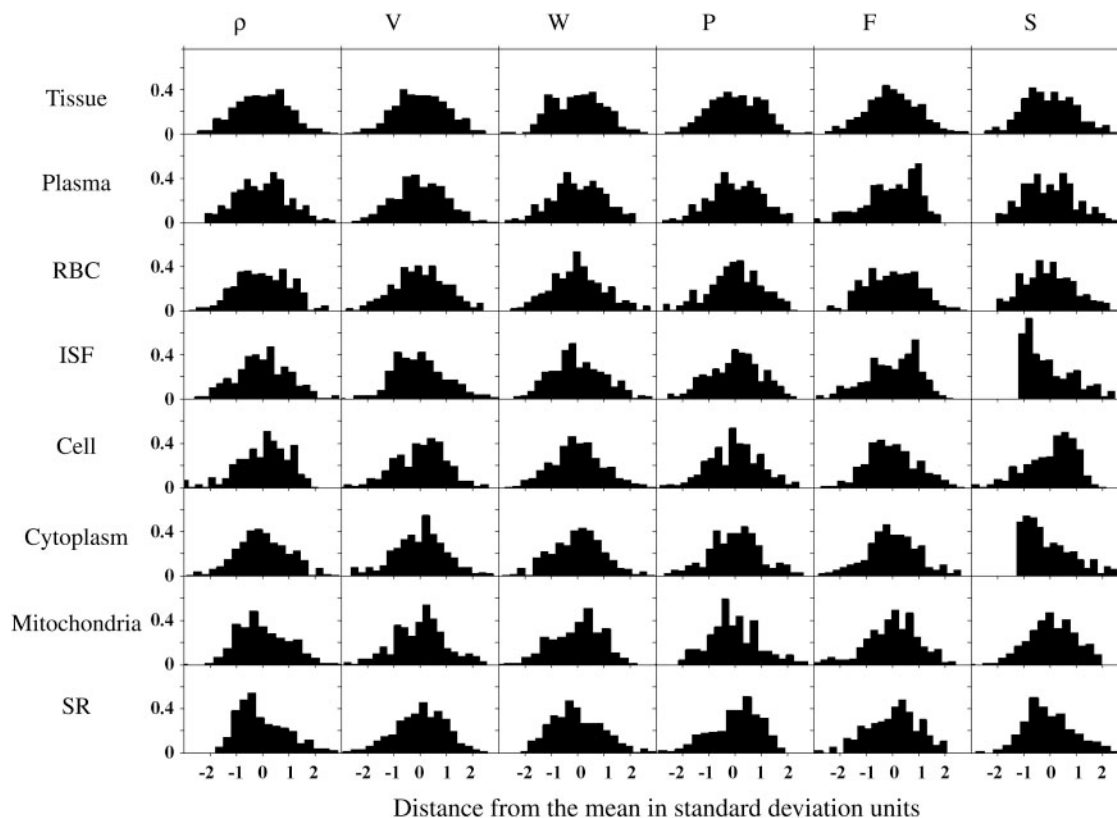
Fig. 2. Probability density functions of composition variables. Each plot is the pdf of the variable listed on the *top* within the region listed on the *left*. The abscissa shows in standard deviation units the distance from the mean of the variable, and the ordinate is the probability density so that the area under each plot is 1. The means and coefficients of variations of the variables are those listed in Table 3. RBC, red blood cell; ISF, interstitial fluid space; SR, sarcoplasmic reticulum.

ficient of variation (CV)] g/ml, negligibly different from the tissue density of 1.0526 g/ml.

Table 4 gives an overview of the mass fractions of the four constituents in the several regions of the tissue, where the values are given as gram per gram organ as a whole. The far right column gives the regional mass as a fraction of the organ mass. For this table, the reference mass is the whole organ including the large vessels. The total solid content of protein + fat + solute is 0.21 g/g. That plus the water fraction (0.79 g/g) accounts for the total mass. The mass fractions for large vessels and microvasculature (the first two values in the far right column) account for 10.7% of the mass, and the ISF accounts for another 16.9%, whereas the cell fraction accounts for the remaining 72.5% of the mass.

Distribution of Water

Table 5 shows water volumes in tissue compartments per gram wet weight of tissue, gram dry weight of tissue, and gram protein in tissue. The cell water mass fraction is 0.56 g/(g organ) but is 0.75 g/(g cell mass) and the cytoplasmic water fraction is yet higher, 0.81 g/(g cytoplasm), from Table 3. Experimentally, metabolite concentrations are measurable in tissue averaged quantities. These volumes will enable the calculation of metabolite concentrations in particular regions of the tissue if it is known where the metabolites are localized. For example, the concentration of a metabolite confined to the mitochondria will be 5.5 times the tissue-averaged concentration. For a metabolite confined to cytosolic water, the actual concentration will be about twice the tissue averaged concentration. This is illustrated in Table 6 for phosphocreatine (PCr) and ATP, two metabolites whose concentrations are usually measured in vivo by using phosphorus NMR detection cali-
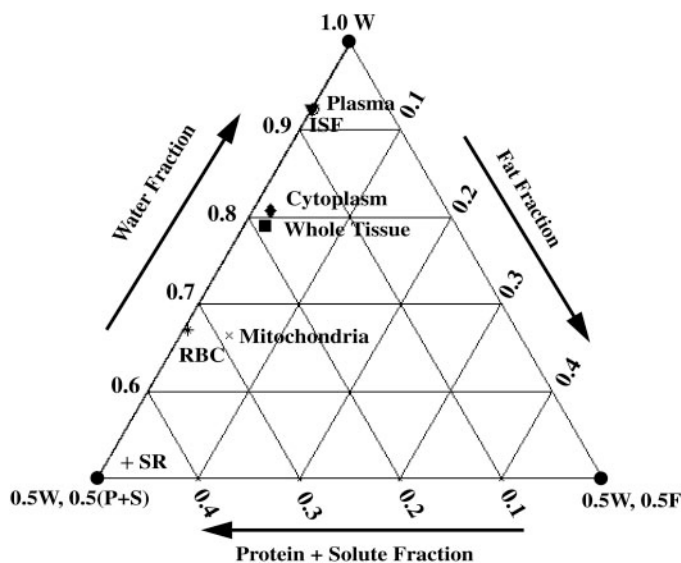
Fig. 3. Observed tissue composition in terms of mass fractions of tissue components. Note the large range of water contents. The SR point is suspiciously low, because it is unlikely to be so dry as this, and more data specific to SR are needed.

Table 4. *Organ constituent mass fractions*

Region	Constituent Masses, g/g organ				
	W	P	F	S	Total g/g organ
Large vessels	0.012	0.0026	0.00005	0.0002	0.015
Microvasculature	0.0757	0.0143	0.0003	0.0014	0.0917
ISF	0.1554	0.0112	0.0002	0.0017	0.1686
Total cell (mi + cy + SR)	0.5469	0.1476	0.02	0.0103	0.7248
Cytoplasm	0.3919	0.0823	0.009	0.0022	0.4853
Mitochondria	0.1409	0.0532	0.0104	0.0077	0.2122
SR	0.0141	0.0121	0.0006	0.0004	0.0272
Total: LV + micro + ISF + cell	0.7901	0.1757	0.0205	0.0137	1.000

brated against solution standards. The concentration of ATP in RBC is 2 mM (28), in cytoplasm it is 16 nmol/mg cell protein, and in the mitochondria it is 4 nmol/mg cell protein (16), which translate into the molar concentrations of Table 6. There is no PCr in normal RBC (18). The rat heart PCr concentration is 39.4 μmol/g dry weight (31), giving 20.8 mM in cytoplasmic water space. The metabolite concentrations are calculated without taking into account any regional variation. The regional variation in metabolite contents is small compared with that of blood flow (15).

DISCUSSION

Although the analytical methods used here are general, mathematically sound, and reliable in the sense of providing reproducibility, and have the benefit of providing confidence limits on all the estimates, it is evident that there is much yet to be learned. We do not yet have a truly comprehensive set of data on any one tissue and thus cannot calculate precise estimates of the subcellular components. Because we are targeting the water content due to its relevance for estimating local driving forces for chemical reactions, we begin the discussion around what are certainly the most accurate and best constrained of the tissue parameters, water fractions.

Water Volumes and Concentrations of Metabolites

This set of data gives the values of regional water spaces, protein, fat, and small molecular solutes (Table 4) per gram of organ, among many other quantities. This enables us to calculate the regional volumes of distribution per gram dry weight of tissue, per gram of total protein, or per gram of mitochondrial protein, the units in which tissue-averaged concentrations are usually obtained in experiments. Volumes of distribution obtained here are necessary to calculate the concentrations of those metabolites having a known regional location.

Tracer dilution studies with [$^{15}OH_2$]water in isolated heart studies (11) using positron emission tomography and tritiated water in isolated dog heart studies (38) would suggest that all of this water is rapidly exchangeable. Such studies affirm the interpretations of Grabowski and Bassingthwaighte (17) and Kellen and Bassingthwaighte (22, 23) who, using osmotic water flux experiments in isolated rabbit hearts, concluded that all the cytosolic and mitochondrial water participates in defining the osmotic gradients driving the water and solute fluxes. The implication is that "bound" water, although it hydrates proteins, is readily exchangeable and participates in dissolving all small solutes, and therefore the total regional water is used for estimating solute concentrations.

From Table 5 we can calculate the ratio of the water space in cytosol to that in mitochondria to be around 2.8. This is significantly different from the volume ratio of 9 from the data in Achs and Garfinkel (1). The data of Randle and Tubbs (31) give the concentrations of metabolites in micromoles per gram dry weight of tissue. For example, the tissue concentration of PCr, given as 39.4 μmol/g dry weight by Randle and Tubbs, corresponds to a cytosolic concentration of 20.8 mM, assuming that PCr is confined to cytosol and is absent from mitochondria. This was calculated by using the value of 1.9 ml cytosolic water/g dry weight from Table 5.

Critique of the Method

Our mass and volume balance analysis for organ and tissue regions distinguishes the composition of plasma, RBC (distributed among the large vessel and microcirculation), ISF, and cells. Cardiomyocytes are the major cell type, but there are other functionally important ones, such as the endothelial cells and smooth muscle cells in the blood vessels. Although the analysis can be readily extended to include more cell types, the critical need is for definitive data on the volume fractions of each, and then on their composition. At the subcellular level,

Table 5. *Water spaces in tissue regions: mean (CV%)*

Region	ml/g tissue	ml/g dry	ml/g protein
Heart	0.792 (0.23)	3.77 (1.1)	4.5 (1.2)
Tissue	0.7917 (0.23)	3.77 (1.1)	4.5 (1.2)
Plasma	0.053 (12.8)	0.25 (12.9)	0.0.3 (12.9)
RBC	0.0243 (36.5)	0.12 (36.5)	0.138 (36.6)
ISF	0.158 (7.1)	0.75 (7.2)	0.9 (7.2)
Cell	0.557 (2.5)	2.65 (2.7)	3.16 (2.7)
Cytoplasm	0.399 (4)	1.9 (4)	2.27 (4.1)
Mitochondria	0.143 (7.6)	0.68 (7.6)	0.82 (76)
SR	0.0143 (3.6)	0.068 (3.8)	0.082 (3.9)

Data are means; values in parentheses are coefficients of variation in %.

Table 6. *Subcellular aqueous concentrations of ATP and PCr*

Region	PCr	ATP
Tissue average	10.45	2.98
Plasma	0	0
RBC	0	2
ISF	0	0
Cytoplasm	20.8	6.03
Mitochondria	0	3.66

Values are given in micrometers. PCr, phosphocreatine.

we have considered mitochondria, sarcoplasmic reticulum, and cytoplasm. This model enabled us to calculate intracellular distribution of water in these three main regions. The cytoplasm includes myofibrils, sarcoplasm, and other organelles such as the nucleus, Golgi bodies, etc. An average density for the whole of this space was assumed on the basis of the X-ray microanalysis measurements of von Zglinicki and Bimmler (34). The densities of the nucleus and other organelles are likely to differ from that of sarcoplasm and myofibrils. The analysis can be expanded to include other organelles that are pertinent but again would require more data to make the refinement meaningful.

The constituent mass fractions in each region are constrained to add up to unity. Solute fraction is mostly constituted by inorganic solutes (mineral). For example, a liter of plasma contains ~11 g of solutes of which 9.4 g are inorganic solutes (36). The inorganic solutes contribute to a large part of osmolarity that is tightly regulated. From a physiological viewpoint, the variance of solute mass fractions is expected to be very small. If these values were constrained by osmotic considerations, they would presumably be closer together because there must be an osmotic balance. Such a balance also includes the cellular protein and its influence on the ionic balance via a Donnan equilibrium. At a next level of model development, inclusion of physiological constraints on solute concentration should reduce the variance in solute mass fractions.

Ideally, all of the data should be collected simultaneously on each heart of a set of hearts in vivo so that the data are completely compatible for each heart. To our knowledge, however, such studies have not been undertaken. We have used data mostly from rats, generating a data set representative of rat myocardium. The results, therefore, represent only a specific example. The method can be applied to any tissue and regions within a tissue.

Another shortcoming is that this analysis does not address the expectation that regional differences in myocardial density must occur secondary to regional differences in mitochondrial volume density, cytoplasmic volume density, and vascular volumes. Such variation is more likely to be evident in the hearts of larger animals. Several studies have shown regional heterogeneity in cardiac functional parameters such as flow, capillary permeability surface area products, and oxygen consumption (10, 15). However, Schaper et al. (33) found no statistically significant differences in organelle volume densities transmurally and regionally in a dog heart. Yipintsoi et al. (39) found no statistically significant differences in the density and water content of the left ventricle, right ventricle, and septum of a dog heart. It is interesting to note the presence of functional heterogeneity despite the homogeneity in anatomy.

Our method required 30,000 iterations to obtain 310 feasible solutions. This is because in each iteration the known variables are assigned values from uncorrelated distributions. But in reality, the tissue composition variables are all correlated with each other because of the mass and volume balance relations. Therefore, only a small set of feasible solutions, in which the variables are correlated, emerge when running our computer program. Distributions of the input variables themselves get filtered to fit the constraints. If all data were taken from the same study, then we would expect the starting distributions and the distributions corresponding to the converged solutions to be the same.

That we see such a high protein density in sarcoplasmic reticulum compared with mitochondria and cytosol, which includes myofibrils and metabolic solutes, raises our suspicions about the accuracy of the calculations. The sarcoplasmic reticulum values are probably the least secure, for we have only the constraint (Table 2) that there is 29.2 mg sarcoplasmic reticulum protein per milliliter cytosol giving us the 0.44 g/g protein fraction. High protein content makes good sense in the light of the high concentrations of Ca pump protein [sarco(endo)plasmic reticulum Ca^{2+}-ATPase] and calsequestrin (Table 25 in Ref. 8). However, we do have a fairly exact estimate of fractional volume of 3.5 ± 0.2% cell volume from Page and McCallister (27). Even so, the estimated water fraction of 0.52 g/g is surprisingly low. Explicit data on sarcoplasmic reticulum are needed to obtain improved estimates.

Densities and Composition

In the present study, the density of tissue was predicted as 1.053 g/ml, which corresponds to that of a sedentary mammal such as the rat, cattle, or human, all of which have heart weight-to-body weight ratios of ~3–5 g/kg. The density of myocardium in these mammals is around 1.055 g/ml (35). The myocardial density is higher in mammals such as the horse and dog, whose heart weight-to-body weight ratios are around 8 g/kg (19, 33) with a value of ~1.06 g/ml (35, 39). These are big differences; a 0.005 difference in density is a 5% difference in buoyancy.

From the observations of Yipintsoi et al. (39), the dog left ventricular myocardium had a density of 1.063 ± 0.002 g/ml with a water fraction of 0.771 g/g tissue and tissue solids constituting the rest. Density of the dog right ventricular myocardium was 1.062 g/ml. From compositional analysis using an average density of 0.901 g/ml for fat and 1.38 g/ml for protein and solutes, they estimated the fat fraction at 0.006 g/g tissue for the dog. For our analysis in rats, we started with a water fraction of 0.79 g/g tissue (4), a fat fraction of 0.0205 g/g tissue from the data of Dible (12), and the remaining as protein and small molecular solutes with a combined density of 1.4 g/ml. This composition yielded an estimated tissue density of 1.053 ± 0.0005 g/ml, significantly lower than that of the dog heart. The question arises as to why dog hearts might be denser than what we estimate for rats in this analysis. We believe that this is due to the species and the conditions of the animals. The dogs were farm dogs and were exercised several times per day in fields, and so were lean and well conditioned. Given that the dog is a running animal with a heart weight-to-body weight ratio of nearly 1% (and even higher in greyhounds), less fat and higher protein levels are to be expected. The sedentary animals serving as the source of our present data had heart weight-to-body weight ratios of ~0.3–0.4%. In affirmation of the notion that running animals have higher myocardial densities, Webb and Weaver (35) report that horse heart density is 1.061 g/ml.

In conclusion, the accumulation of myocardial data that we gathered mostly from rats, combined with a mathematical approach to forcing the data into a set of self-consistent estimates of density, water content, volume, and mass fractions gives us a firm and rather reliable way of describing tissue composition. The method can be applied to any tissue, and is best applied to detailed data sets from organs of a specific species rather than a collection from diverse species. The

representation would be made more precise by having more explicit detail on tissue components and subcellular regions, but even without those refinements, the representation gives fairly narrowly defined limits on the volume and mass fractions.

REFERENCES

1. **Achs MJ and Garfinkel D.** Computer simulation of energy metabolism in anoxic perfused rat heart. *Am J Physiol Regul Integr Comp Physiol* 232: R164–R174, 1977.
2. **Aliev MK, Dos Santos P, Hoerter JA, Soboll S, Tikhonov AN, and Saks VA.** Water content and its intracellular distribution in intact and saline perfused rat hearts revisited. *Cardiovasc Res* 53: 48–58, 2002.
3. **Allen TH, Krzywicki HJ, and Roberts JE.** Density, fat, water and solids in freshly isolated tissues. *J Appl Physiol* 14: 1005–1008, 1959.
4. **Altman PL and Dittmer DS (Editors).** *Metabolism.* Bethesda, MD: Federation of American Societies for Experimental Biology, 1968, p. 737.
5. **Altman PL and Dittmer DS (Editors).** *Respiration and Circulation.* Bethesda, MD: Federation of American Societies for Experimental Biology, 1971, p. 930.
6. **Barth E, Stammler G, Speiser B, and Schaper J.** Ultrastructural quantitation of mitochondria and myofilaments in cardiac muscle from 10 different animal species including man. *J Mol Cell Cardiol* 24: 669–681, 1992.
7. **Bassingthwaighte JB, Raymond GR, and Chan JIS.** Principles of tracer kinetics. In: *Nuclear Cardiology: State of the Art and Future Directions,* edited by Zaret BL and Beller GA. St. Louis, MO: Mosby-Year Book, 1993, p. 3–23.
8. **Bers DM.** *Excitation-Contraction Coupling and Cardiac Contractile Force* (2nd ed.). Dordrecht, The Netherlands: Kluwer Academic, 2001, p. 427.
9. **Brozek J, Grande F, Anderston JT, and Keys A.** Densitometric analysis of body composition: revision of some quantitative assumptions. *Ann NY Acad Sci* 110: 113–140, 1963.
10. **Caldwell JH, Martin GV, Raymond GM, and Bassingthwaighte JB.** Regional myocardial flow and capillary permeability-surface area products are nearly proportional. *Am J Physiol Heart Circ Physiol* 267: H654–H666, 1994.
11. **Deussen A and Bassingthwaighte JB.** Modeling [^{15}O]oxygen tracer data for estimating oxygen consumption. *Am J Physiol Heart Circ Physiol* 270: H1115–H1130, 1996.
12. **Dible JH.** Is fatty degeneration of the heart muscle a phanerosis? *J Pathol Bacteriol* 39: 197–207, 1934.
13. **Dobson GP and Cieslar JH.** Intracellular, interstitial and plasma spaces in the rat myocardium in vivo. *J Mol Cell Cardiol* 29: 3357–3363, 1997.
14. **Effros RM and Chinard FP.** The in vivo pH of the extravascular space of the lung. *J Clin Invest* 48: 1983–1996, 1969.
15. **Franzen D, Conway RS, Zhang H, Sonnenblick EH, and Eng C.** Spatial heterogeneity of local blood flow and metabolite content in dog hearts. *Am J Physiol Heart Circ Physiol* 254: H344–H353, 1988.
16. **Geisbuhler T, Altschuld RA, Trewyn RW, Ansel AZ, Lamka K, and Brierley GP.** Adenine nucleotide metabolism and compartmentalization in isolated adult rat heart cells. *Circ Res* 54: 536–546, 1984.
17. **Grabowski EF and Bassingthwaighte JB.** Capillary transport and exchange: an osmotic weight transient model for estimation of capillary transport parameters in myocardium. In: *Microcirculation Proceedings of the First World Congress for the Microcirculation,* edited by Grayson J and Zingg W. New York: Plenum, 1976, vol. 2, p. 29–50.
18. **Griffiths WJ.** Creatine and phosphocreatine in the human red cell. *Br J Haematol* 15: 389–399, 1968.
19. **Hoppeler H, Lindstedt LS, Claassen H, Taylor RC, Mathieu O, and Weibel ER.** Scaling mitochondrial volume in heart to body mass. *Respir Physiol* 55: 131–137, 1984.
20. **Idell-Wenger JA, Grotyohann LW, and Neely JR.** Coenzyme A and carnitine distribution in normal and ischemic hearts. *J Biol Chem* 253: 4310–4318, 1978.
21. **Judd RM and Levy BI.** Effects of barium-induced cardiac contraction on large- and small-vessel intramyocardial blood volume. *Circ Res* 68: 217–225, 1991.
22. **Kellen MR and Bassingthwaighte JB.** An integrative model of coupled water and solute exchange in the heart. *Am J Physiol Heart Circ Physiol* 285: H1303–H1316, 2003.
23. **Kellen MR and Bassingthwaighte JB.** Transient transcapillary exchange of water driven by osmotic forces in the heart. *Am J Physiol Heart Circ Physiol* 285: H1317–H1331, 2003.
24. **Klitzman B and Duling BR.** Microvascular hematocrit and red cell flow in resting and contracting striated muscle. *Am J Physiol Heart Circ Physiol* 237: H481–H490, 1979.
25. **Méndez J and Keys A.** Density and composition of mammalian muscle. *Metabolism* 9: 184–188, 1960.
26. **Norseth J, Normann PT, and Flatmark T.** Hydrodynamic parameters and isolation of mitochondria, microperoxisomes and microsomes of rat heart. *Biochim Biophys Acta* 719: 569–579, 1982.
27. **Page E and McCallister LP.** Quantitative electron microscopic description of heart muscle cells. *Am J Cardiol* 31: 172–181, 1973.
28. **Pennell RB.** Composition of Normal Human Red Cells. *The Red Blood Cell,* edited by Surgenor DM. New York: Academic, 1974, vol. 1, p. 93–146.
29. **Pries AR, Secomb TW, and Gaehtgens P.** Biophysical aspects of blood flow in the microvasculature. *Cardiovasc Res* 32: 654–667, 1996.
30. **Prinzen FW and Bassingthwaighte JB.** Blood flow distributions by microsphere deposition methods. *Cardiovasc Res* 45: 13–21, 2000.
31. **Randle PJ and Tubbs PK.** Carbohydrate and fatty acid metabolism. In: *Handbook of Physiology, The Cardiovascular System. The Heart.* Bethesda, MD: Am. Physiol. Soc., 1979, sect. 2, vol. I, chapt. 23, p. 805–844.
32. **Sarelius IH and Duling BR.** Direct measurement of microvessel hematocrit, red cell flux, velocity, and transit time. *Am J Physiol Heart Circ Physiol* 243: H1018–H1026, 1982.
33. **Schaper J, Meiser E, and Stämmler G.** Ultrastructural morphometric analysis of myocardium from dogs, rats, hamsters, mice, and from human hearts. *Circ Res* 56: 377–391, 1985.
34. **Von Zglinicki T and Bimmler M.** The intracellular distribution of ions and water in rat liver and heart muscle. *J Microsc* 146: 77–85, 1987.
35. **Webb AI and Weaver BMQ.** The density of equine tissue at 37°C. *Res Vet Sci* 26: 71–75, 1979.
36. **White A, Handler P, Smith EL, Hill RL, and Lehman IR.** *Principles of Biochemistry.* New York: McGraw-Hill, 1978.
37. **Wiig H, Reed RK, and Tenstad O.** Interstitial fluid pressure, composition of interstitium, and interstitial exclusion of albumin in hypothyroid rats. *Am J Physiol Heart Circ Physiol* 278: H1627–H1639, 2000.
38. **Yipintsoi T and Bassingthwaighte JB.** Circulatory transport of iodoantipyrine and water in the isolated dog heart. *Circ Res* 27: 461–477, 1970.
39. **Yipintsoi T, Scanlon PD, and Bassingthwaighte JB.** Density and water content of dog ventricular myocardium. *Proc Soc Exp Biol Med* 141: 1032–1035, 1972.